



BRILL

## COMPLEMENTARY IMAGING TECHNIQUES FOR CHARCOAL EXAMINATION AND IDENTIFICATION

Wannes Hubau<sup>1,2,3</sup>, Jan Van den Bulcke<sup>1,2</sup>, Peter Kitin<sup>3</sup>, Loes Brabant<sup>2,4</sup>,  
Joris Van Acker<sup>1,2,\*</sup> and Hans Beeckman<sup>3</sup>

<sup>1</sup>Ghent University, Department of Forest and Water Management, Laboratory of Wood Technology,  
Coupure Links 653, B-9000 Gent, Belgium

<sup>2</sup>Ghent University, Centre for X-ray Tomography (UGCT), Proeftuinstraat 86, B-9000 Gent, Belgium

<sup>3</sup>Royal Museum for Central Africa, Laboratory for Wood Biology, Leuvensesteenweg 13,  
B-3080 Tervuren, Belgium

<sup>4</sup>Ghent University, Department of Physics and Astronomy, Proeftuinstraat 86, B-9000 Gent, Belgium

\*Corresponding author; e-mail: joris.vanacker@ugent.be

### ABSTRACT

Identification of ancient charcoal fragments is a valuable tool in reconstructing past environments and determining natural and anthropogenic disturbances, and for understanding past cultures and societies. Although in Europe such studies are fairly straightforward, utilising charcoal records from the tropics is more complicated due to the species-richness of the natural vegetation. Comprehensive databases have greatly aided identification but often identification of charcoali-fied woods from the tropics relies on minute anatomical features that can be difficult to observe due to preservation or lack of abundance.

This article illustrates the relative potential of four imaging techniques and discusses how they can provide optimal visualisation of charcoal anatomy, such that specific difficulties encountered during charcoal examination can be evaluated and fine anatomical characters can be observed enabling high-level identification of charcoal (and wood) taxa. Specifically reflected Light Microscopy is often used to quickly group large numbers of charcoal fragments into charcoal types. Scanning Electron Microscopy and High-Throughput X-ray Computed Tomography are employed to observe fine anatomical detail. More recently X-ray Computed Tomography at very high resolution has proved successful for imaging hidden or ‘veiled’ anatomical features that cannot be detected on exposed surfaces but need three-dimensional volumetric imaging.

**Keywords:** Archaeobotany, X-ray Computed Tomography, SEM, RLM, wood anatomy, xylem, charcoal identification.

### INTRODUCTION

Identification of radiocarbon dated charcoal fragments from soil profiles or archaeological excavations is valuable in assessing past vegetation and climate change. Moreover charcoali-fied wood can provide great insights into the relative importance of wood types to past cultures and ancient societies. Charcoal analysis is regularly practised in

Europe and North Africa where the vegetation is relatively species-poor and identification to at least genus level using Reflected Light Microscopy (RLM) and/or Scanning Electron Microscopy (SEM) is often possible (*e.g.* Carcaillet & Thinon 1996; Figueiral & Mosbrugger 2000; Gale & Cutler 2000; Scheel-Ybert 2000; Di Pasquale *et al.* 2008; Théry-Parisot *et al.* 2010; Höhn & Neumann 2012; Schweingruber 2012). However, identification of (ancient) charcoal fragments from species-rich biomes such as Central Africa is often challenging. Large databases such as InsideWood (2012) and the Tervuren Xylarium Wood Database (2012; the world's largest reference collection of Central African wood specimens) have greatly aided such systematic identifications (Wheeler 2011; Hubau *et al.* 2012) but difficulties involving interspecific anatomical similarity and intraspecific anatomical variability are often encountered, which hamper wood and charcoal identification (Normand & Paquis 1976; Gasson 1987; Schweingruber 2007).

Moreover the process of charcoalification coupled with post-depositional processes can lead to fractures, deformities or impurities that can obscure anatomical features. One example is the formation of coatings on vessel walls that originate from non-wood related deposits such as minerals and fungal hyphae (*e.g.* Prior & Gasson 1993; Figueiral & Mosbrugger 2000; Scheel-Ybert 2000; Scott 2000; Scott & Glasspool 2007; Bird *et al.* 2008; Braadbaart & Poole 2008; Di Pasquale *et al.* 2008; Dias Leme *et al.* 2010; Théry-Parisot *et al.* 2010; Ascough *et al.* 2011). Charcoal is also brittle in nature and fragments are traditionally hand-fractured (Gale & Cutler 2000) for observation under Reflected Light Microscopy (RLM) and Scanning Electron Microscopy (SEM). If clean surfaces are required, time-consuming embedding methods and an extremely stable microtome are needed to make thin sections (Schweingruber 1976, 2012). Complementary imaging techniques can help overcome such problems associated with preservation and sample preparation in the study of charcoal anatomy.

Conventionally Reflected Light Microscopy is employed for grouping large numbers of fragments into different 'charcoal types', which are presumed to be from the same woody taxon (*e.g.* Carcaillet & Thinon 1996; Chabal *et al.* 1999; Höhn & Neumann 2012; Hubau *et al.* 2012). The samples are hand-fractured or fractured with the help of a razor blade which often renders surfaces damaged and not always clean enough to return the necessary detailed anatomical information. Experienced anthracologists can break, mount, observe and group up to 100 well-preserved fragments from the tropics each day using this approach.

High-Throughput X-ray Computed Tomography (HT- $\mu$ CT) and Scanning Electron Microscopy are more time-consuming and expensive than RLM because they require sample preparation, operating time and output handling. SEM enables detailed visualisation of fine anatomical characters (*e.g.* Boutain *et al.* 2010) but only about five charcoal fragments can be prepared and imaged in one day (although timings vary depending upon requirement and preservation). SEM is subject to the same surface observation constraints as RLM but gives the most detailed images possible at this time and is compatible with HT- $\mu$ CT. In turn, HT- $\mu$ CT allows unlimited slicing of a three-dimensional scan of a charcoal fragment providing clean digital 'cuts' comparable to thin sections (Van den Bulcke *et al.* 2009; Mannes *et al.* 2010). However, HT- $\mu$ CT does not allow

visualisation of details such as septae or intervessel pits, and batch preparation, scanning, reconstruction, observation and reslicing together take about two working days for ten charcoal fragments.

X-ray Computed Tomography at very high resolution (nanotomography, or nanoCT) is a valuable tool for imaging minute features that are not clearly visible on surface cuts under RLM or SEM. For example, when visibility is obscured by coatings on vessel walls a directed search in three-dimensional nanoCT volumes provides images of the structures beneath the deposits or coatings by digitally cutting through them (*e.g.* Van den Bulcke *et al.* 2009; Mannes *et al.* 2010).

This article outlines the potential of these four imaging techniques for charcoal identification and discusses how they are able to contribute to a better visualisation of the fine anatomical features needed to identify material from species-rich biomes such as Central African rainforests.

## METHODOLOGY

### Charcoal sampling and grouping in charcoal types

The material used in this study originates from the Mayumbe, a submountainous chain covered by semi-deciduous tropical rainforests stretching along the Atlantic coast from Gabon down to the Democratic Republic of Congo. The edges of the forest are vulnerable to fragmentation caused by human activities and past climate anomalies and charcoal records help in the quantification and qualification of such disturbances (Ngomanda *et al.* 2009; Colombaroli & Verschuren 2010; Picornell Gelabert *et al.* 2011; Hubau *et al.* 2012). Charcoal fragments were sampled from seven soil profiles excavated in the southern Mayumbe forest in the Lower Congo Province, Democratic Republic of Congo (between 04° 30' S and 06° 00' S and between 12° 30' E and 13° 30' E; see Hubau *et al.* 2012). The charcoal fragments were cleaned, hand-fractured, and mounted on 'Plastillin' (see Carcaillet & Thinon 1996; Scheel-Ybert 2000; Di Pasquale *et al.* 2008 for further details). The fragments from each profile were then grouped into distinct anatomical charcoal types using RLM.

### Imaging and describing charcoal types

One representative fragment, measuring approximately 10 mm<sup>3</sup>, of each charcoal type was mounted on a stub, sputter-coated with gold and subsequently observed under SEM (JSM-6610LV; JEOL, Tokyo, Japan) with an accelerating voltage of 10 kV.

Two representative charcoal fragments for each charcoal type were selected for High-Throughput X-ray Computed Tomography (HT- $\mu$ CT) with an approximate voxel pitch of 2.5  $\mu$ m (*e.g.* Van den Bulcke *et al.* 2009; Mannes *et al.* 2010). The scanner, built at Ghent University Centre for X-ray Tomography ([www.ugct.ugent.be](http://www.ugct.ugent.be)), is similar to the one described by Masschaele *et al.* (2007) and Van den Bulcke *et al.* (2009) and has a generic CT scanner control software platform (Dierick *et al.* 2010). The fragments were glued into small plastic tubes each with a diameter of 3 mm. These tubes are able to hold up to ten charcoal fragments and can be scanned as one batch overnight (Van den Bulcke *et al.* 2009). All reconstructions were performed in 'Octopus', a tomography reconstruction package for parallel, cone-beam and helical geometry (Vlassenbroeck

*et al.* 2007). Virtual sample rotation and reslicing was carried out with Morpho+ (Brabant *et al.* 2011).

If anatomical details such as intervessel pits or vessel-ray pits were found to be unclear under RLM, SEM or HT- $\mu$ CT, a small fragment (< 0.9 mm) containing a vessel or a vessel grouping was accurately cut using a scalpel under RLM and mounted individually on a small stub. The fragment was then scanned using nanoCT with an approximate voxel pitch of 0.65  $\mu$ m. Three-dimensional volumes were digitally visualised (= rendered, see Van den Bulcke *et al.* 2009) using the software package VGStudio Max. Exploring these 3D volumes for anatomical details requires time, experience and a customised treatment. On some occasions, several prospective short (> 30 min) scans (and reconstructions) of different samples were performed before the desired minute anatomical features (*e.g.* pits) could be found. Since the samples cannot be scanned in one batch nanoCT is more time-consuming (two to five samples a day) than either SEM or HT- $\mu$ CT and is thus reserved for samples in which the details of specific anatomical features are required for identification and cannot be determined from another technique. For each charcoal type descriptions were made in accordance with the on-line InsideWood database (IAWA Committee 1989; Wheeler 2011; InsideWood 2012). The final description for each charcoal type consisted of two strings of numbered features. The first string represents primary features that are easily visible. The second string represents secondary features that are variable or unclear.

### Identifying charcoal types

All charcoal types were identified to the highest taxonomic level wherever possible by applying the Central African charcoal identification methodology of Hubau *et al.* (2012). This method was developed using an umbrella database of species names and metadata compiled from the on-line InsideWood Database (InsideWood 2012) and the Tervuren Xylarium Wood Database (2012) in addition to inventory and indicator species lists (*e.g.* Lebrun & Gilbert 1954). This Central African charcoal identification methodology enables a directed search taking into account metadata on (i) anatomical features, (ii) availability of thin sections within the Tervuren reference collection, (iii) species distribution, and (iv) synonymy. Identification begins with an anatomical query within this database, followed by automatic extension and reduction phases of the resulting species list and ends with a comparative microscopic study of the anatomy of the charcoal type in comparison with thin sections of reference wood samples from the Tervuren Xylarium Wood Database (for a detailed description see Hubau *et al.* 2012). Following these identification phases, one or more species from the database were retained and the charcoal type assigned a 9-character code featuring the first three letters of the family, genus and species name of one of the retained species (*e.g.* ANA PSE MIC stands for Anacardiaceae, *Pseudospondias microcarpa* (A. Rich.) Engl.).

### Recognising and evaluating specific problems encountered with the Central African charcoal identification methodology

Four specific problems were encountered when identifying the charcoal types from the Mayumbe soil profiles: (i) anatomical similarity amongst different charcoal types,

(ii) inadequate matches between charcoal anatomy and reference wood samples, (iii) varying degree of anatomical similarity exhibited by fragments assigned to one particular charcoal type, and (iv) poor preservation of charcoal anatomy. An evaluation system for each of these obstacles is defined in Table 1 and discussed more fully below.

The problem of anatomical similarity amongst different charcoal types arises during the grouping of the fragments into charcoal types using RLM. Charcoal types either resembled other types from different soil profiles or resembled a second type within the same profile (see Table 1). The evaluation criterion can be split into two categories namely ‘+++’ for a clear distinction between one charcoal type and the other types, or ‘--’ for a degree of similarity shared with the one charcoal type under study and at least one other type (Table 1).

The second problem, *i.e.* inadequate match between a charcoal type and reference wood samples housed in the Tervuren xylarium, occurs during the comparative phase. After identification, the wood species (one or more) that show closest anatomical similarity to the charcoal type are retained and an ‘anatomy rank’ assigned to that charcoal type. This rank reflects the degree of similarity between the anatomy of the charcoal type under study and that of the reference material. A ranking system is used where +++ and ++ equate to an ‘almost perfect match’ with respectively two or more than two species. Furthermore + and - equate to a ‘moderate match’ with respectively two or more than two species. Finally -- indicates a poor match with the reference material (see Table 1). The preferred outcome would be that the charcoal type under study matches just one extant species almost perfectly (*i.e.* rank +++). However, more usually identification rests with a group of species (*i.e.* several retained species, ranks ++ or -). The inability to identify the charcoal type to a single species reflects that the anatomy of several species within one genus simply do not possess distinct anatomical features that can be used to separate them. This inability hampers palaeobotanical interpretation especially when the retained species have varying habitat preferences (see also Höhn & Neumann 2012).

The third problem, *i.e.* varying degree of anatomical similarity exhibited by fragments assigned to a particular charcoal type, occurs when charcoal fragments from both juvenile and mature wood are present or when stem wood and distorted branch axil wood are both represented. The evaluation criterion is divided into two categories, namely +++ when all fragments in one charcoal type are similar and -- when discrepancies occur within the charcoal type (Table 1).

The fourth problem encountered is that concerning the preservation of the fine anatomical features needed for identification. Structural modifications of the anatomy can occur prior to charcoalification, during the charcoalification process itself or from limited post-depositional processes which can affect the degree of preservation (or ‘clarity’). The charcoal clarity classes are distinguished based on the relative clarity of the representative fragments examined under SEM and HT- $\mu$ CT and in particular the visibility of intervessel pits (see Table 1 for details). Briefly, charcoal anatomy can be regarded as very clear if most features are clearly visible and is thus ranked as +++ or ++; it is moderately clear (+ or -) or very unclear (--) if respectively some or most features (*e.g.* ray cells) are obscured or distorted due to fissures, coatings etc.

Table 1. Evaluation of the four specific problems, (1)–(4), encountered during the identification of twelve charcoal types from a species-rich biome in Central Africa (Mayumbe, DRC). For each problem encountered the charcoal types were assigned an evaluation class ranging from +++ to -- (see text for further details). →

---

## RESULTS AND DISCUSSION

### Selected charcoal types and evaluation of the four problems encountered

From the seven profiles excavated, 84 charcoal types were identified. Table 1 presents 12 charcoal types used to illustrate the four problematic criteria discussed above and the evaluation with each charcoal type. Anatomical similarity amongst different charcoal types is frequently encountered as confirmed by ten of the 12 charcoal types studied here (Table 1). These ten types resemble more than two other charcoal types whilst the remaining two charcoal types resemble only one other type. These two charcoal types attaining a +++ rank exhibit a distinct combination of anatomical characters: ANA PSE MIC has very large ray cells combined with aliform parenchyma and large intervessel pits (7–10 µm) representing an almost perfect match with *Pseudospondias micrantha*. APO ANC PYR has large vessels, laticifers and uniseriate rays and matches *Ancylobotrys pyriformis* almost perfectly.

With regard to inadequate matches between charcoal anatomy and reference wood samples following identification, the charcoal types generally receive a ranking of either very good (+++ and ++) or moderate (+ and -) suggesting that good matches are often made between reference wood samples and charcoal types. However, even though matches are good, there are usually more than two matching species retained (*i.e.* ++ and - in Table 1), preventing identification to species level.

Varying degree of anatomical similarity exhibited by fragments assigned to a particular charcoal type and poor preservation of charcoal anatomy both appear to be less important than the first two problems encountered (Table 1). This implies that charcoal fragments assigned to a certain charcoal type resemble the representative charcoal fragment used for SEM and HT-µCT and that the charcoal anatomy was relatively well-preserved.

Table 1 allows the distinction between successful and less successful identifications by comparing the evaluation results for each of the four problems encountered. For example, charcoal type APO ANC PYR has obtained a good score for each of the four problems. This charcoal type has a very distinct anatomy and resembles only one species perfectly. Conversely, charcoal type RUB AID MIC scores badly or moderately for each of the four problems with some charcoal fragments seeming to differ from the representative fragments used for SEM and HT-µCT, and charcoal anatomy is poorly preserved. This type resembles one other charcoal type in the same soil profile and five charcoal types in other profiles. Furthermore, seven species were retained after identification including *Aidia micrantha* (occurring in primary rainforest), *Euclinia longiflora* (from secondary rainforest) and *Tricalysia pallens* and *Gardenia ternifolia* (both from woodland savanna) (Burkill 1985; African Plants Database 2012). As such, it is unclear from which vegetation type charcoal type RUB AID MIC might have originated.



Charcoal type	Fig.	evaluation of problems				Family name	Retained species
		(1)	(2)	(3)	(4)		
ANA PSE MIC	1,2	+++	+++	+++	++	Anacardiaceae	<i>Pseudospondias microcarpa</i> (A. Rich.) Engl.
APO ANC PYR	5	+++	+++	+++	+++	Apocynaceae	<i>Ancylbothrys pyriformis</i> Pierre
ANN ANN LEB	3	--	-	+++	+++	Annonaceae	<i>Annickia lebrunii</i> (Robyns & Ghesq.) Setten & Maas
						Annonaceae	<i>Xylopia phloioidora</i> Mildbr.
						Annonaceae	<i>Xylopia rubescens</i> Oliv.
						Annonaceae	<i>Xylopia staudtii</i> Engl. & Diels
ANN XYL AUR	3	--	-	+++	+++	Annonaceae	<i>Xylopia parviflora</i> (A. Rich.) Benth.
						Annonaceae	<i>Xylopia villosa</i> Chipp.
						Annonaceae	<i>Xylopia aurantioidora</i> De Wild. & T. Durand
						Annonaceae	<i>Xylopia gilbertii</i> Boutique
						Annonaceae	<i>Xylopia katangensis</i> De Wild.
ANN XYL HYP	4	--	++	+++	+++	Annonaceae	<i>Xylopia cupularis</i> Mildbr.
						Annonaceae	<i>Xylopia hypolampra</i> Mildbr.
						Annonaceae	<i>Xylopia toussaintii</i> Boutique
						Annonaceae	<i>Xylopia katangensis</i> De Wild.
ANN XYL AET	4	--	+	--	+++	Annonaceae	<i>Xylopia aethiopica</i> (Dunal) A. Rich.
RUB NAU SPP	7	--	-	--	+	Rubiaceae	<i>Nauclea diderrichii</i> (De Wild.) Merr.
						Rubiaceae	<i>Nauclea vanderghuchtii</i> (De Wild.) E.M.A. Petit
						Rubiaceae	<i>Sarcocephalus latifolius</i> (Sm.) Bruce
						Rubiaceae	<i>Sarcocephalus pobeguini</i> Pobeg.
MYR SYZ GUI	8	--	-	--	+	Moraceae	<i>Ficus louisii</i> Lebrun & Boutique ex Boutique & J.Léonard
						Myrtaceae	<i>Syzygium guineense</i> (Willd.) DC.
						Moraceae	<i>Syzygium staudtii</i> (Engl.) Mildbr.
RUB COR SPP	9	--	-	+++	++	Rubiaceae	<i>Ficus cordata</i> Thunb.
						Rubiaceae	<i>Corynanthe pachyceras</i> K. Schum.
						Rubiaceae	<i>Corynanthe paniculata</i> Welw.
						Rubiaceae	<i>Pausinystalia johimbe</i> Pierre ex Beille
						Rubiaceae	<i>Pausinystalia talbotii</i> Wernham
						Rubiaceae	<i>Pausinystalia zenkeri</i> W. Brandt
CAE GUI SPP	10	--	++	+++	+	Caesalpinioideae	<i>Hallea rubrostipulata</i> (K. Schum.) J.-F.Leroy
						Caesalpinioideae	<i>Craterispermum triflora</i> (K. Schum.) Thonn.
						Caesalpinioideae	<i>Guibourtia arnoldiana</i> (De Wild. & T. Durand) J. Léonard
						Caesalpinioideae	<i>Guibourtia demusei</i> (Harms) J. Léonard
RUB AID MIC	10	--	-	--	--	Caesalpinioideae	<i>Guibourtia ehie</i> (A. Chév.) J. Léonard
						Caesalpinioideae	<i>Guibourtia pellegriniana</i> J. Léonard
						Caesalpinioideae	<i>Guibourtia coleosperma</i> (Benth.) J. Léonard
						Rubiaceae	<i>Aidia micrantha</i> (K. Schum.) Bullock ex F.White
						Rubiaceae	<i>Euclina longiflora</i> Salisb.
						Rubiaceae	<i>Chomelia flaviflora</i> Hutch. & Dalz.
CAE AFZ SPP	6	--	++	+++	+++	Rubiaceae	<i>Gardenia ternifolia</i> Schumach. & Thonn.
						Rubiaceae	<i>Leptactinia arboldiana</i> De Wild.
						Rubiaceae	<i>Tricalysia pallens</i> Hiern
						Rubiaceae	<i>Tricalysia aequatoria</i> E. Robbrecht
						Caesalpinioideae	<i>Afzelia bella</i> Harms
						Caesalpinioideae	<i>Afzelia bipindensis</i> Harms
Caesalpinioideae	<i>Afzelia pachyloba</i> Harms						
Caesalpinioideae	<i>Afzelia africana</i> Sm.						
Caesalpinioideae	<i>Afzelia peturei</i> De Wild.						
Caesalpinioideae	<i>Afzelia quanzensis</i> Welw.						

(1) Anatomical similarities amongst different types

+++ similarity with no or only one other type  
 -- similarity with two or more other types

(2) Inadequate match between charcoal type and reference material

+++ almost perfect match with only one species  
 ++ almost perfect match with more than one species  
 + moderate match with only one species  
 - moderate match with more than one species  
 -- poor match with one or more species

(3) Variability within a charcoal type

+++ all fragments belonging to the charcoal type are similar  
 -- some fragments seem to differ from others belonging to the same type

(4) Poor preservation of charcoal anatomy

+++ general anatomy and intervessel pits very clear  
 ++ general anatomy very clear but intervessel pits unclear, requiring nanoCT  
 + general anatomy moderately clear and intervessel pits clearly visible  
 - general anatomy moderately clear and intervessel pits unclear, requiring nanoCT  
 -- general anatomy very unclear

Table 2. Comparative overview of the four microscopy techniques in relation to specific observation goal important for the charcoal identification process.

	Reflected Light Microscopy	Scanning Electron Microscopy	High-throughput X-ray Computed Tomography	High-resolution X-ray Computed Tomography
	RLM	SEM	HT- $\mu$ CT	nanoCT
<b>Observation goal</b>	grouping in types	detailed description	detailed description	3D directed search of details
<b>Process</b>				
sample preparation	hand-fracturing	hand-fracturing	hand-fracturing/cutting	hand-fracturing/cutting
mounting on sample holder	orientation on plastillin	orientation on stub	batch preparation	accurate mounting on stub
device operation	—	gold-coating + vacuum	overnight batch scanning	one by one scanning
output handling	—	—	reconstruction	reconstruction
output handling	—	—	reslicing (Morpho+)	rendering (VG Studio Max)
<b>Speed</b> (# fragments per day)	100 day <sup>-1</sup>	5 day <sup>-1</sup>	5 day <sup>-1</sup>	2–5 day <sup>-1</sup>
<b>Obtained detail</b>				
magnification	up to 100 ×	up to 4000 × or more	—	—
resolution	—	—	voxel pitch = 2.5 $\mu$ m	voxel pitch = 0.65 $\mu$ m
<b>Trade-offs</b>				
Strengths	fast initial phase, used for grouping in types, but not for imaging	sharp, detailed visualisation	unlimited reslicing, clear observation planes (digital thin sections)	imaging 'hidden' features, combined observation of planes
Current limitations	unclear observation planes due to hand-fracturing	unclear observation planes due to hand-fracturing	low resolution	experienced manipulation & customised treatment



### Complementary imaging

An overview of the four microscopy techniques is presented in Table 2 in relation to image process, speed, detail obtained and trade-offs. Reflected Light Microscopy was only used for fast grouping of charcoal fragments into types. It was not used for

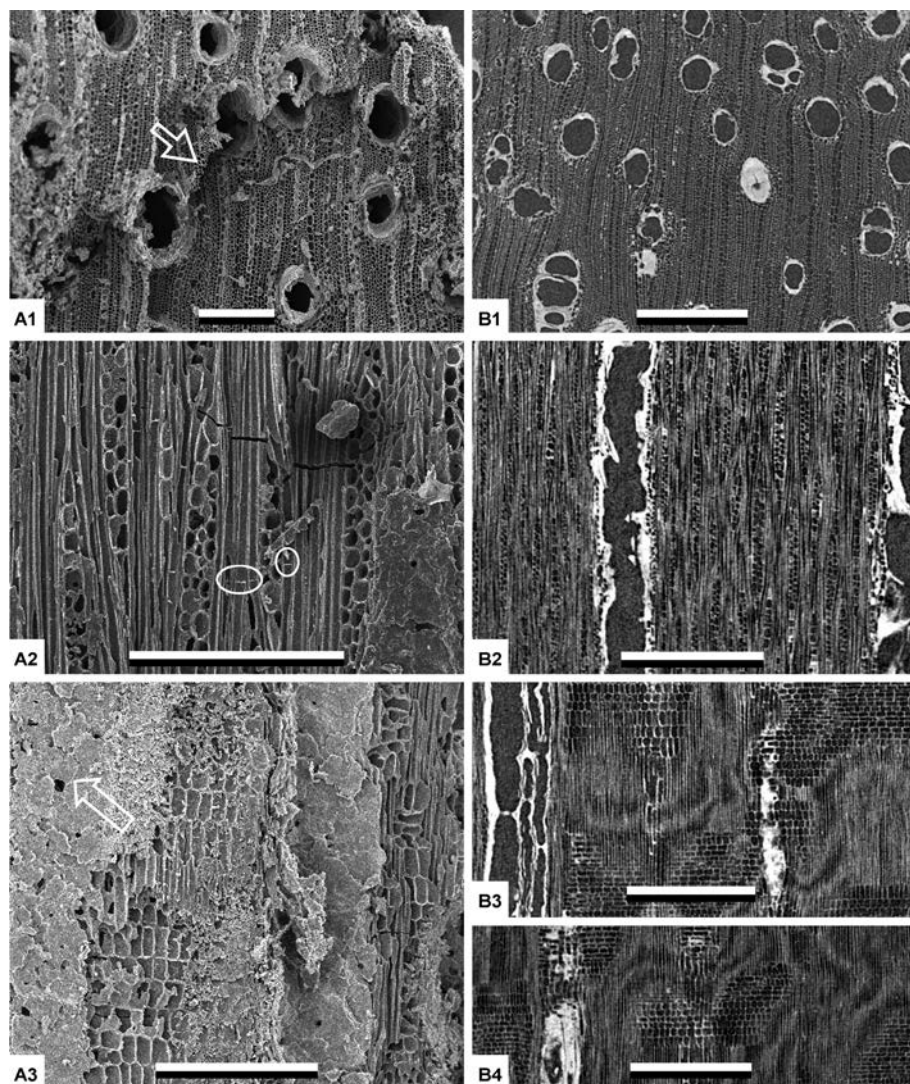


Figure 1. Illustration of SEM and HT- $\mu$ CT as two complementary imaging techniques on charcoal type ANA PSE MIC. – A1–A3: SEM images of ANA PSE MIC – A1: TS – A2: TLS – A3: RLS. Note tangential fissure (arrowed in A1) probably caused by hand fracturing; fibre septae (encircled in A2); unclear surface probably caused by sample preparation (arrowed in A3) obscuring large parts of the rays. Scale bars = 200  $\mu$ m. – B1–B4: HT- $\mu$ CT images of ANA PSE MIC fragment 1. – B1: TS – B2: TLS – B3: RLS. Note large parts of the ray are now visible (compare to A3). Scale bars = 500  $\mu$ m.

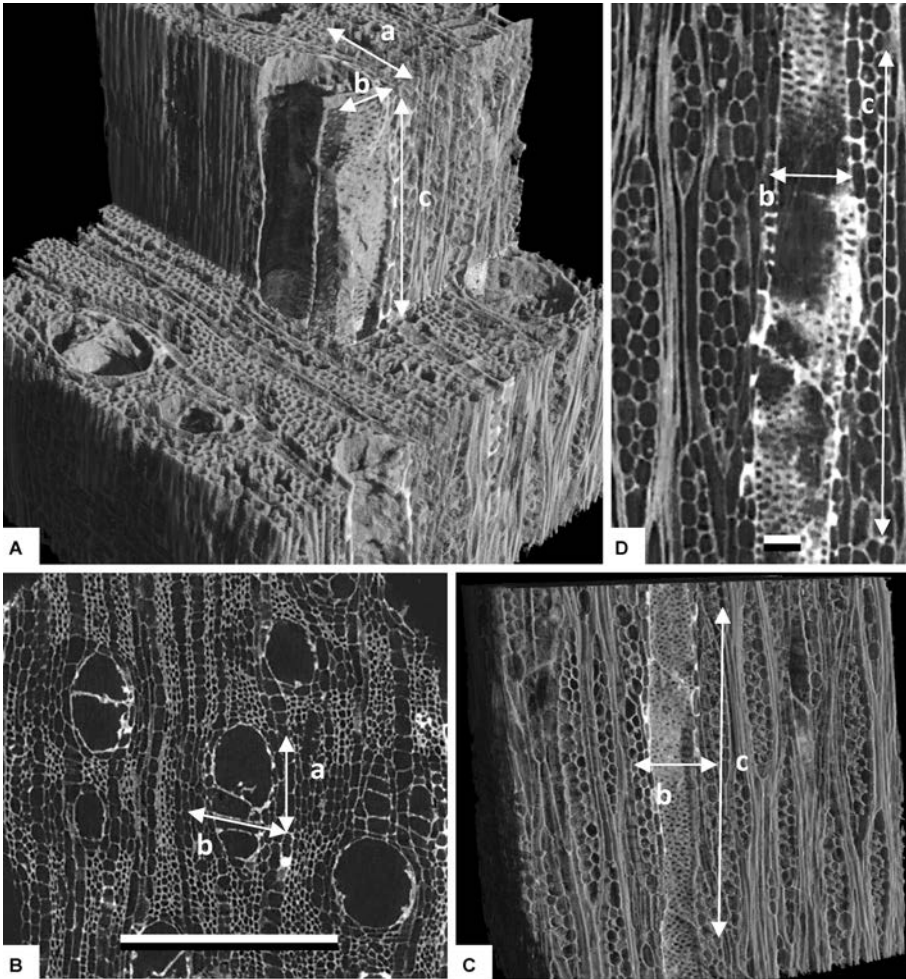


Figure 2. Illustration of how obscured interessel pits can be visualised using nanoCT by targeting a less well-coated interessel wall on which the interessel pits can be located by ‘cutting’ through digital 3D volumes. – a: Vessel alignment; b: Targeted interessel wall; c: Interessel pits on vessel element. – A: three-dimensional volume. – B: TS; scale bar = 200  $\mu\text{m}$ . – C: Three-dimensional volume. – D: TLS (detail of interessel pits); scale bar = 20  $\mu\text{m}$ .

imaging because the surfaces of the Mayumbe specimens were mostly not flat and the anatomy sometimes damaged.

SEM (Fig. 1A) and HT- $\mu\text{CT}$  (Fig. 1B) imaging are highly compatible. Yet even though SEM can provide sharpness and fine detail (*e.g.* septae in Fig. 1A2) an important disadvantage of SEM is the possible damage caused through hand fracturing (*e.g.* Boutain *et al.* 2010) (Fig. 1A1 and 1A3). Often radial longitudinal sections are very unclear (*e.g.* Fig. 1A3). Conversely HT- $\mu\text{CT}$  is a non-destructive visualisation technique (*e.g.* the clear transverse section illustrated in Fig. 1B1) allowing the production of virtual



volumes that can be resliced in any direction, often revealing a complete view of the ray structure (Fig. 1 B3). HT- $\mu$ CT allows almost unlimited ‘slicing’ of the charcoal sample (compared with the one section on offer with SEM) (cf. Van den Bulcke *et al.* 2009). This is illustrated in Figure 1 B4 which presents a second radial HT- $\mu$ CT image of the

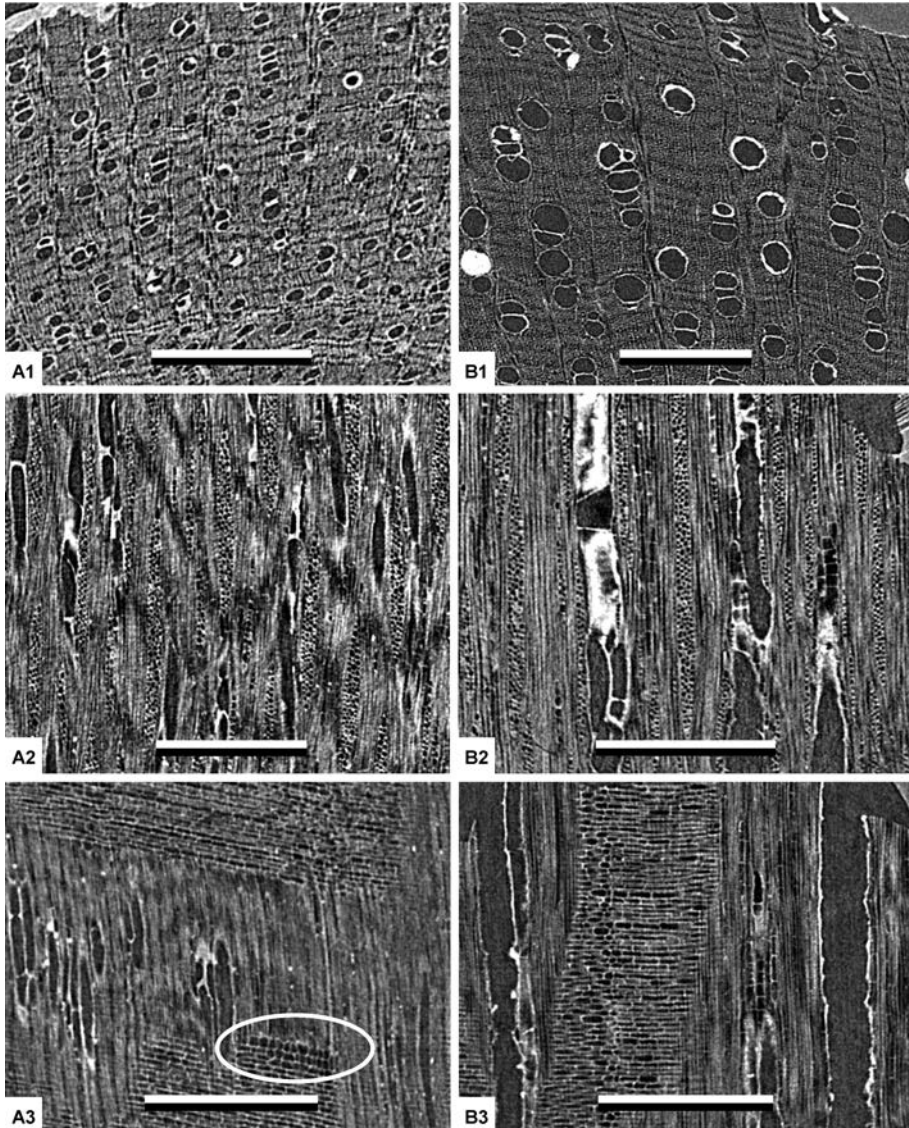


Figure 3. Illustration of two resembling charcoal types belonging to the Annonaceae. – A1–A3: HT- $\mu$ CT images of charcoal type ANN ANN LEB. – A1: TS with vessel groupings circled – A2: TLS – A3: RLS with upright marginal ray cells circled. – Scale bars = 400  $\mu$ m. – B1–B3: HT- $\mu$ CT images of charcoal type ANN XYL AUR. – B1: TS with vessel groupings circled – B2: TLS – B3: RLS. – Scale bars = 500  $\mu$ m.

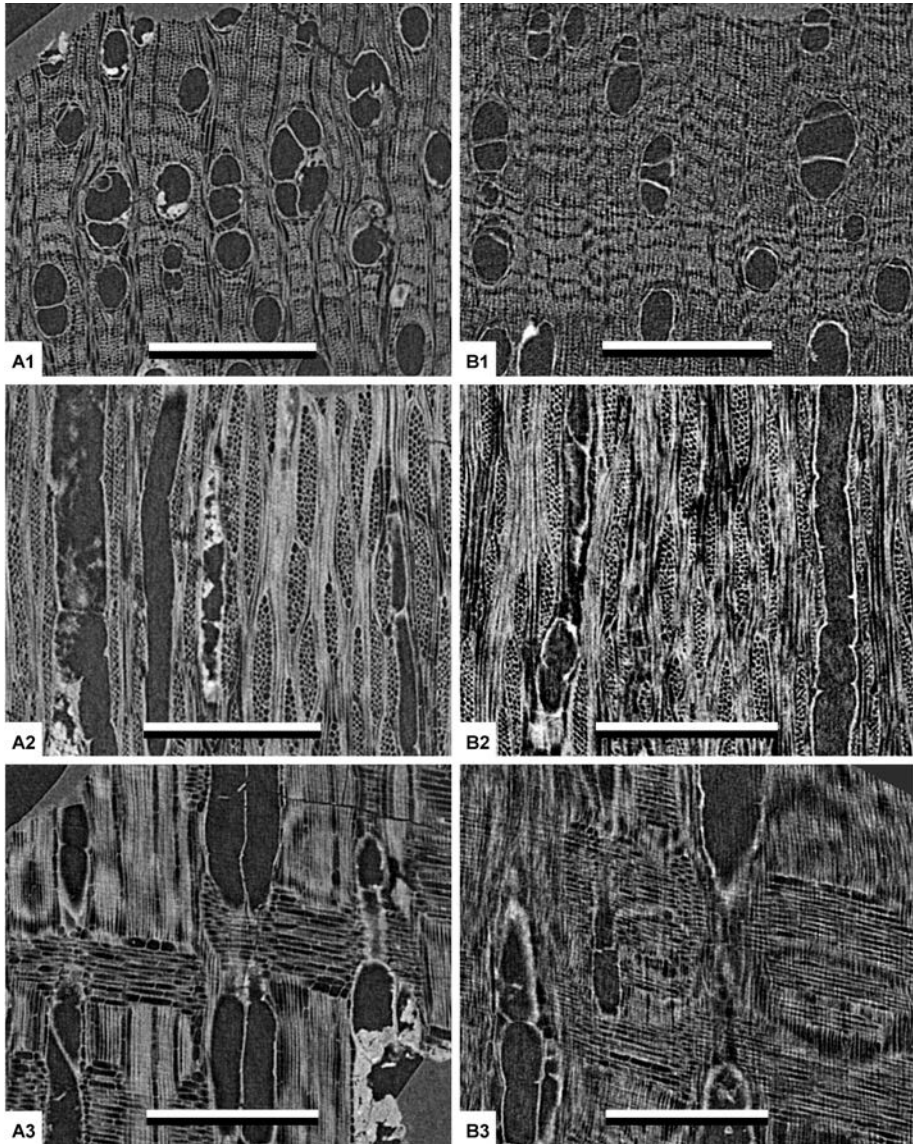


Figure 4. Illustration of two resembling charcoal types belonging to the Annonaceae. – A1–A3: HT- $\mu$ CT images of charcoal type ANN XYL HYP. – A1: TS with vessel grouping circled – A2: TLS – A3: RLS. – Scale bars = 500  $\mu$ m. – B1–B3: HT- $\mu$ CT images of charcoal type ANN XYL AET. – B1: TS with vessel groupings circled – B2: TLS – B3: RLS. – Scale bars = 500  $\mu$ m.

same charcoal fragment shown in Figure 1 B3. However, the resolution of HT- $\mu$ CT is not as high as in SEM and fibre septae and pits are not visible. The HT- $\mu$ CT images presented here have a voxel pitch of approximately 2.5  $\mu$ m (Table 2), which allows visualisation of cells but not of sub-cellular details.



Details such as vessel-ray pitting or intervessel pitting can also be difficult to detect under SEM. For example most of the vessel walls in charcoal type ANA PSE MIC are covered with an unidentified deposit – probably non-wood-related mineral particles (vessels in Fig. 1A and Fig. 1B). In this case a small charcoal fragment containing a group of vessels with fewer deposits (Fig. 2B) was isolated using RLM and scanned with nanoCT, which incorporates the advantages of both HT- $\mu$ CT and SEM but does require skilled manipulation, and batch processing is not yet feasible (*e.g.* Van den Bulcke *et al.* 2009; Mannes *et al.* 2010). A directed search in reconstructed nanoCT volumes can locate intervessel walls and intervessel pits (Fig. 2A) and provide a 3D reconstruction of the charcoal type focusing on a group of vessels (indicated by ‘a’ in Fig. 2). More specifically, an intervessel wall has been targeted on Figure 2 (indicated by ‘b’). Intervessel pits are clear on 3D images (indicated by ‘c’ in Fig. 2A and 2C), but they can also be found on re-sliced 2D images if the volume is rotated appropriately in Morpho+ (indicated by ‘c’ in Fig. 2D). While studying 3D volumes it is possible to combine several observation planes (*e.g.* Fig. 2A where transverse, tangential and radial planes have been combined into one image) thus obtaining a better understanding of the 3D anatomical structure. Conversely, 2D images offer the opportunity to undertake precise measurements of minute characters such as intervessel pits through the use of scale bars (*e.g.* Fig. 2D where the approximate intervessel pit size is about 6 or 7  $\mu$ m).

## Visualisation of the four problems encountered

### *Anatomical similarities amongst charcoal types*

Different woody species belonging to the same family or genus can be difficult or even impossible to differentiate simply on their anatomy alone. For example, three charcoal types (RUB NAU SPP, RUB COR SPP and RUB AID MIC) listed in Table 1 belong to the Rubiaceae, the fourth largest angiosperm family (Mabberley 2008) in which morphological and anatomical similarities complicate taxonomy and identification. Each of these three charcoal types resembles at least three other types belonging to the Rubiaceae, in some cases from the same soil profile. This is further exemplified by the Annonaceae. All species retained after identification of charcoal types ANN ANN LEB, ANN XYL HYP, ANN XYL AUR and ANN XYL AET are assigned to this family (Table 1). Figure 3 and 4 present HT- $\mu$ CT images of these four charcoal types and clearly illustrate the similarities between ANN ANN LEB (Fig. 3A) and ANN XYL AUR (Fig. 3B) thus complicating the decision to merge these charcoal types or to keep them separate. Both these types have uniseriate bands of axial parenchyma, small groups of radially aligned vessels (Fig. 3 A1 and 3 B1), and relatively wide (four or more cells) and long (> 1 mm) rays (Fig. 3 A2 and 3 B2). However, ANN ANN LEB has clearly one or two rows of upright marginal ray cells (Fig. 3 A3), a feature lacking in ANN XYL AUR (Fig. 3 B3). The other Annonaceae types, ANN XYL HYP and ANN XYL AET, also resemble ANN ANN LEB and ANN XYL AUR, although ANN XYL HYP and ANN XYL AET have fewer radial vessel alignments and larger vessels (Fig. 4 A1 and 4 B1). ANN XYL HYP seems to have a slightly higher incidence of vessel groupings relative to ANN XYL AET but otherwise these types are difficult to distinguish from each other.

***Inadequate match between charcoal anatomy and reference wood samples***

Ideally one charcoal type will only match one woody species from the reference collection almost perfectly (evaluation ‘+++’ in Table 1) but in reality only a few genera have species with anatomical features characteristic enough to enable identification to this level. This ‘perfect match’ was found with charcoal type APO ANC PYR (Fig. 5) where laticifers in the rays enabled such a match (Fig. 5 A2 and B2). If IAWA fea-

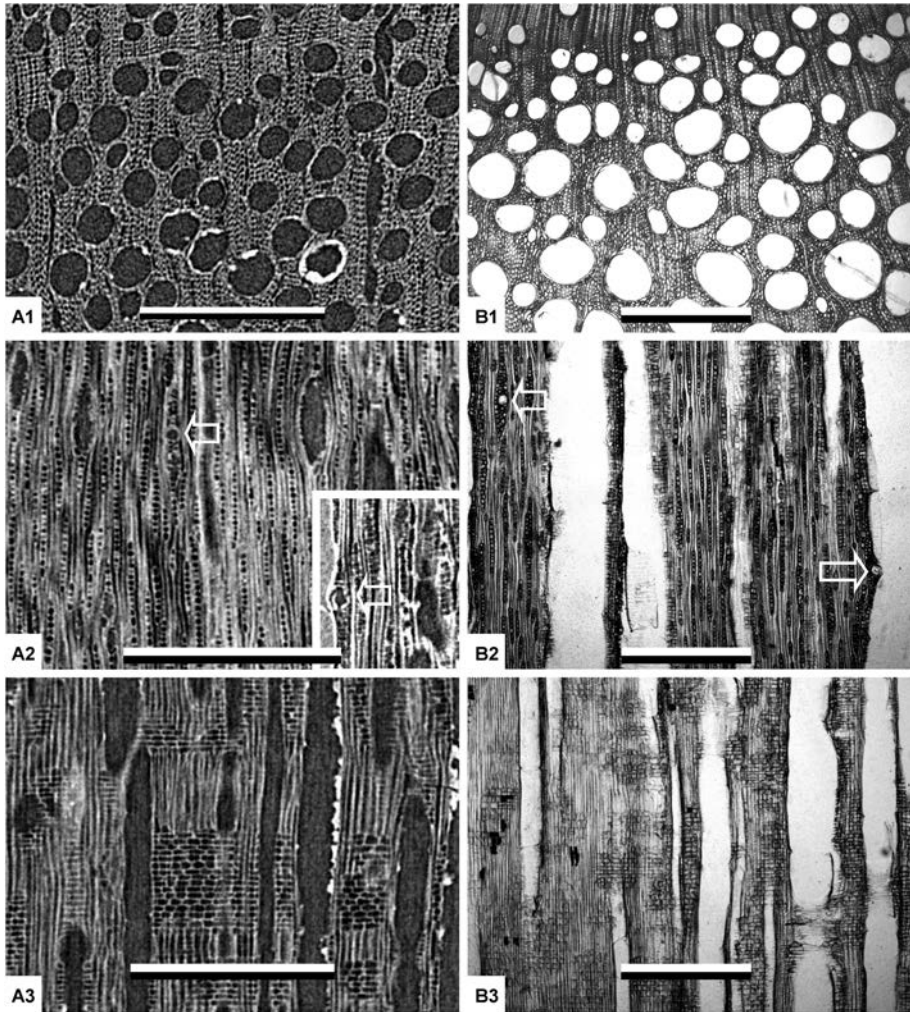


Figure 5. Illustration of a very successful identification with an almost perfect match between charcoal type (APO ANC PYR) and reference material and only one best matching species. – A1–A3: HT- $\mu$ CT images of APO ANC PYR. – A1: TS – A2: TLS with laticifers arrowed – A3: RLS. – Scale bars = 500  $\mu$ m. – B1–B3: Transmitted light micrographs of a thin section of a reference wood sample (Tw 34886) of *Ancylobotrys pyriformis*. – B1: TS – B2: TLS with laticifers arrowed and inset showing intervessel pit detail (scale bar = 10  $\mu$ m) – B3: RLS. – Scale bars = 500  $\mu$ m.

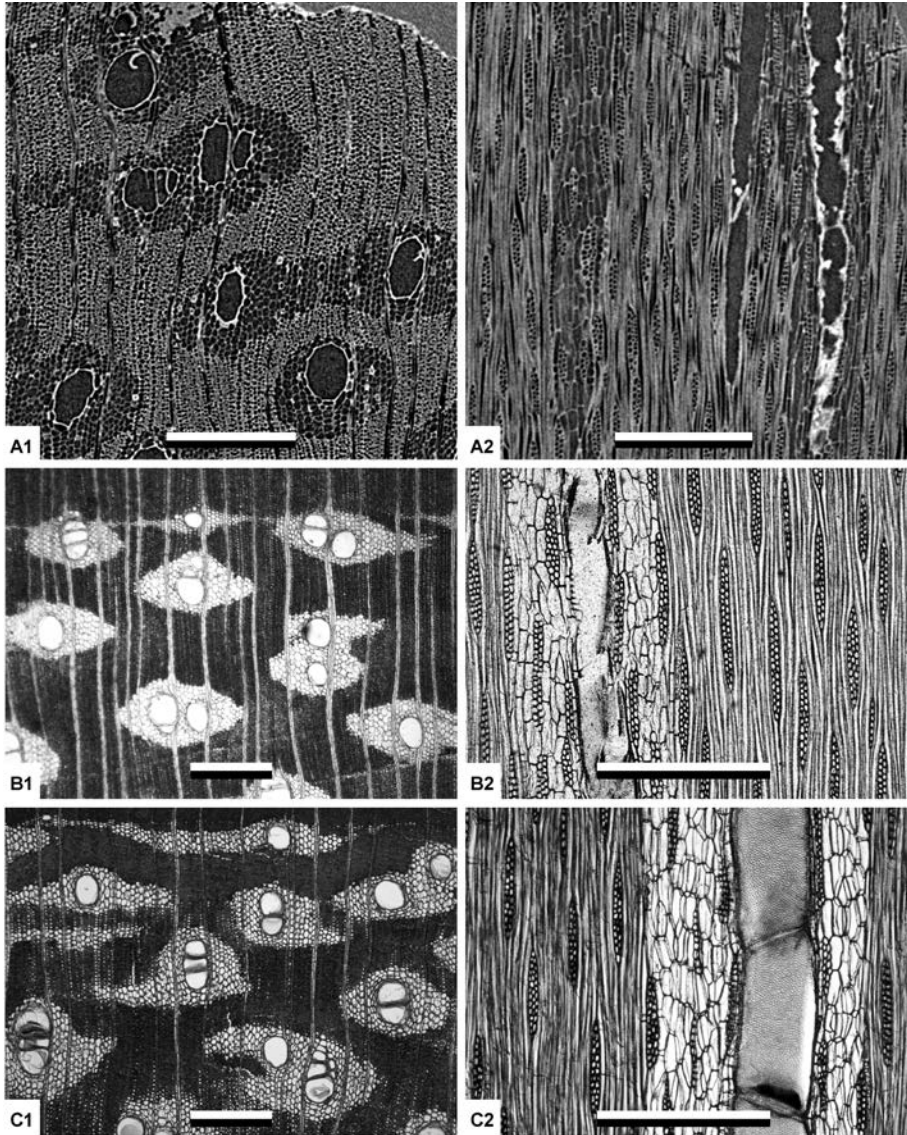


Figure 6. Illustration of one charcoal type resembling several extant woody species. – A1–A2: HT- $\mu$ CT images of charcoal type CAE AFZ SPP. – A1: TS – A2: TLS. – Scale bars = 400  $\mu$ m. – B1–B2: Transmitted light micrographs of thin sections of a reference wood sample (Tw 45137) of *Afzelia bella*. – B1: TS – B2: TLS. – Scale bars = 500  $\mu$ m. – C1–C2: Transmitted light micrographs of a thin section of a reference wood sample (Tw 2417) of *Afzelia bipindensis*. – C1: TS – C2: TLS. – Scale bars = 500  $\mu$ m. – B1–C2 illustrate the similarity between modern species in this genus.



tures 132r and 179r are used together on the on-line InsideWood Database, only 17 Central African species with laticifers are found (Wheeler *et al.* 2007; Wheeler 2011; InsideWood 2012). Charcoal type APO ANC PYR is thus distinct from all other charcoal types in this study. The vessels are solitary, very large (150–250  $\mu\text{m}$ ) and abundant (25–32 per  $\text{mm}^2$ ) (Fig. 5 A1 and 5 B1), similar to those of lianas (Carlquist 1991; Angyalossy *et al.* 2011). Rays are uniseriate but sporadically multiseriate when they contain laticifers (Fig. 5 A2 and 5 B2). Charcoal images are very similar to thin sections of the liana *Ancylotryps pyriformis* housed in the modern reference collection (Fig. 5B).

More usually, however, charcoal types match more than just one woody species, thus preventing identification to species level. This is the case for charcoal type CAE AFZ SPP, which matches six *Afzelia* species (Table 1). HT- $\mu\text{CT}$  images of this charcoal type are presented in Figure 6A and compared with transmitted light images of reference wood samples of two different *Afzelia* species from the Tervuren Xylarium Wood Database (2012) (Fig. 6B and 6C). These species of *Afzelia* help to illustrate the problem with differentiating between certain species using wood anatomy (see also Normand & Paquis 1976).

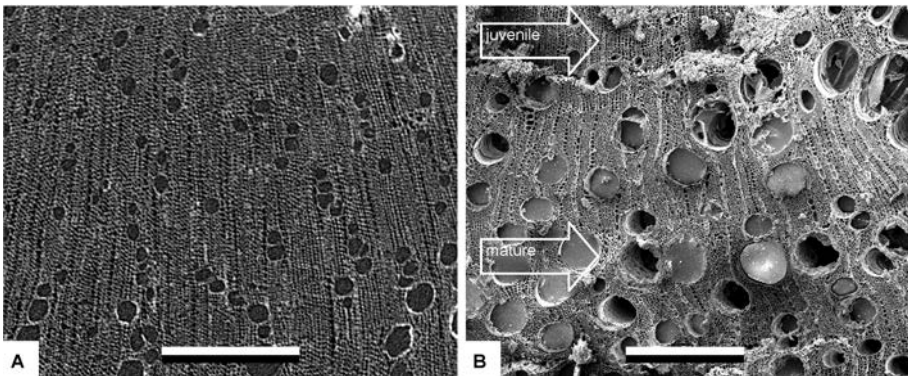


Figure 7. Anatomical variability in fragments belonging to the same charcoal type (RUB NAU DID). – A: HT- $\mu\text{CT}$  image of juvenile wood (TS) exhibited by a first charcoal fragment. – B: SEM image (TS) of a second charcoal fragment showing both juvenile and mature anatomy. – All scale bars = 400  $\mu\text{m}$ .

#### ***Anatomical variability in fragments belonging to the same charcoal type***

Anatomy of trees and shrubs of the same species can vary significantly between individuals or even within the same individual depending on the age, presence of traumatic tissue and distorted wood in branch axils (*e.g.* Gasson 1987; Carlquist 1988; Schweingruber 2007). In this study such anatomical variations were also found. Charcoalified juvenile wood is represented by fragments of charcoal type RUB NAU SPP (Fig. 7) characterised by the presence of pith tissue in some fragments (not shown) and converging rays (Fig. 7A). Figure 7B represents both mature and juvenile wood

in one fragment of the same charcoal type. A further example is illustrated by different fragments of charcoal type MYR SYZ GUI found from the same soil profile. One fragment appears to be derived from distorted wood (Fig. 8A) whereas the second (Fig. 8B) shows typical mature wood anatomy.

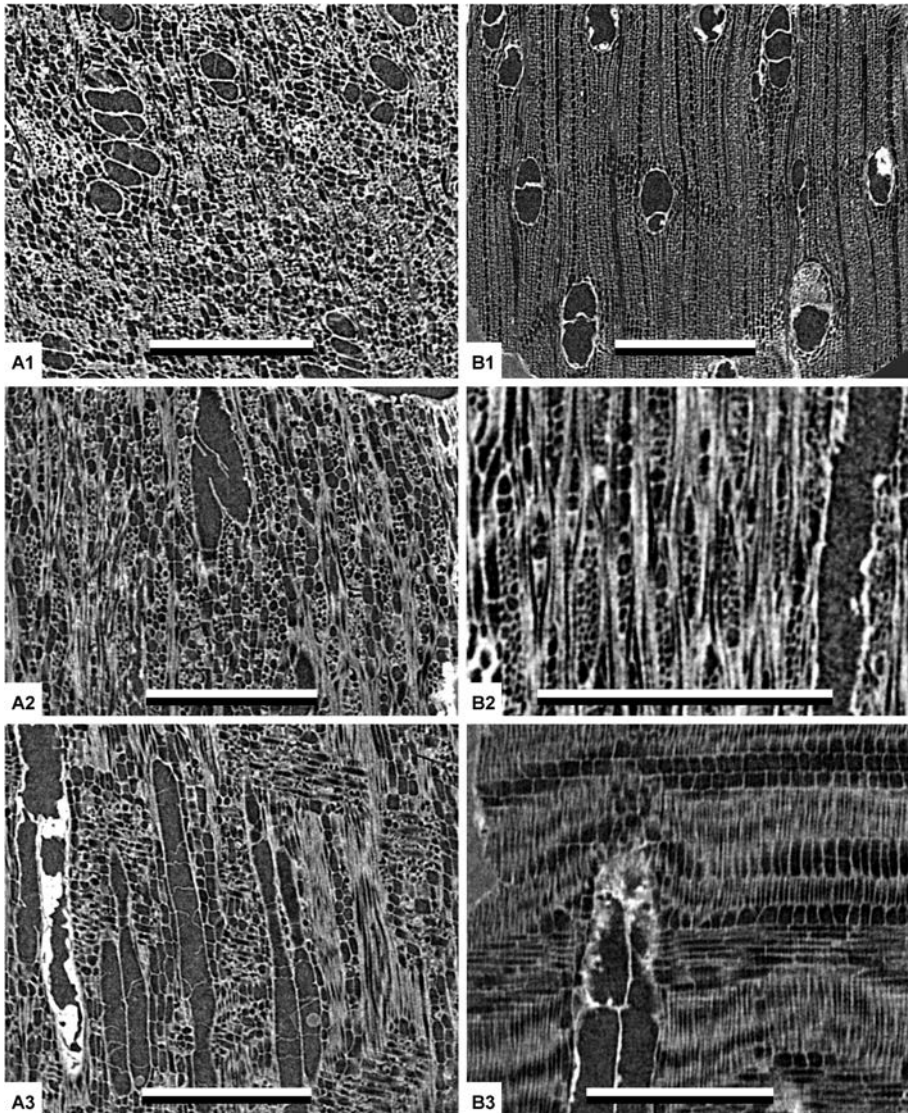


Figure 8. Anatomical variability in fragments belonging to the same charcoal type. – A1–A3: HT- $\mu$ CT images of charcoal type MYR SYZ GUI (fragment 1) showing distorted anatomy. – A1: TS – A2: TLS – A3: RLS. – B1–B3: HT- $\mu$ CT images of charcoal type MYR SYZ GUI (fragment 2) showing typical mature wood anatomy for comparison. – B1: TS – B2: TLS – B3: RLS. – All scale bars = 500  $\mu$ m.

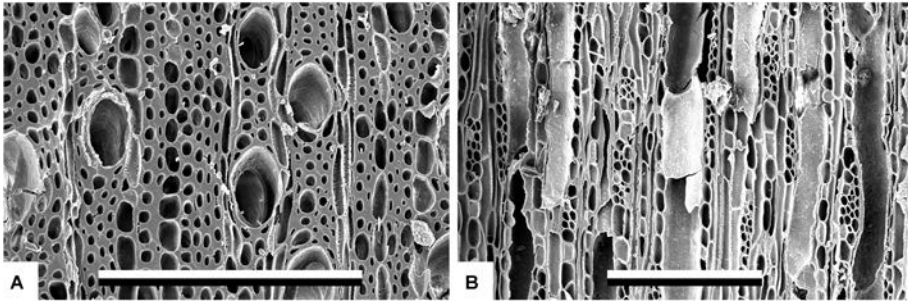


Figure 9. Illustration of ‘very clear’ charcoal anatomy preservation as illustrated by charcoal type RUB COR SPP (SEM images). – A: TS – B: TLS. – Scale bars = 200  $\mu\text{m}$ .

### **Poor preservation of charcoal anatomy**

Often charcoal is very well-preserved anatomically and classified as ‘very clear’ in Table 1 (*e.g.* charcoal type RUB COR SPP in Fig. 9). Yet sometimes charcoal can show areas of distortion and/or fusion probably as a result of the exposure temperature during the charcoalification process (*e.g.* charcoal type CAE GUI SPP in Fig. 10A) (Braadbaart & Poole 2008) and is classified as ‘moderately clear’ (Table 1). Other fragments exhibit ‘very unclear’ (Table 1) charcoal anatomy. This is exemplified by charcoal type RUB AID MIC exhibiting noticeable splits or fractures (Fig. 10 B1) possibly forming as a result of a long heating time during charcoalification or exposure to a high temperature (Braadbaart & Poole 2008; Dias Leme *et al.* 2010), which can also result in the shrinkage of some anatomical features such as vessel diameter (Prior & Gasson 1993; Braadbaart & Poole 2008).

## CONCLUSION

Charcoal identification involves understanding and evaluating a number of specific problems pertaining to the preserved anatomy. This article discusses four such problems, namely (i) anatomical similarity amongst different charcoal types, (ii) inadequate matches between charcoal anatomy and reference thin sections of modern woody species, (iii) anatomical variability amongst fragments assigned to one charcoal type, and (iv) poor preservation of charcoal anatomy. Although these problems often impede high taxonomic identification, complementary imaging techniques can improve identification success especially when the charcoal under study comes from a species-rich biome (*e.g.* Central Africa).

Reflected Light Microscopy (RLM) is advantageous in the grouping of large numbers of anatomically distinct charcoal fragments. Scanning Electron Microscopy (SEM) and High-Throughput X-ray Computed Tomography (HT- $\mu\text{CT}$ ) are highly compatible and fast visualisation techniques. SEM can provide high resolution imaging necessary for detailed anatomical study. However, the observation field under SEM is limited to small exposed areas on the surface of the sample and anatomical characteristics can be lost due to damage caused by hand-fracturing in sample preparation. Contrast HT- $\mu\text{CT}$  offers less detail but does allow unlimited non-destructive ‘reslicing’ of the charcoal



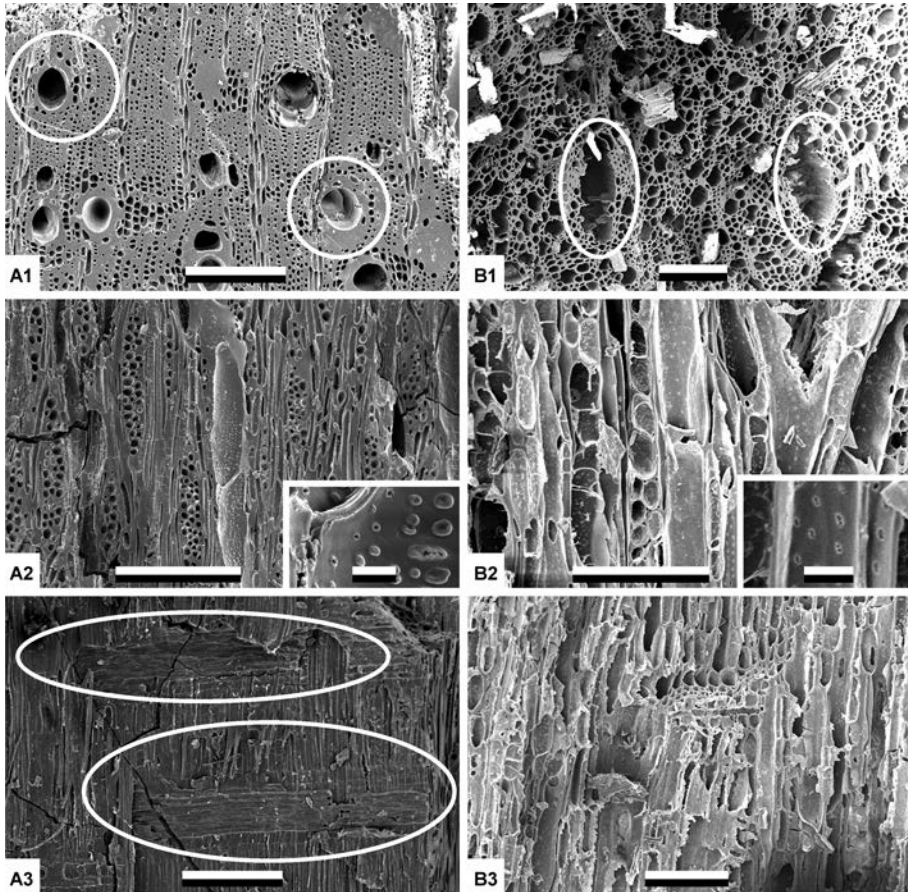


Figure 10. Illustration of ‘moderately clear’ and ‘unclear’ charcoal anatomy preservation. – A1–A3: SEM images of ‘moderately clear’ anatomy as illustrated by charcoal type CAE GUI SPP with seemingly fused aliform parenchyma (circled in A1) and fused ray parenchyma cells (circled in A3); inter vessel pit detail is still visible (A2 inset, scale bar = 10  $\mu\text{m}$ ). – A1: TS – A2: TLS – A3: RLS. – Scale bars = 200  $\mu\text{m}$ . – B1–B3: SEM images of ‘very unclear’ anatomy as illustrated by charcoal type RUB AID MIC with cracks (circled in B1) caused by the charcoalification process; inter vessel pit detail can still be visible (B2 inset, scale bar = 10  $\mu\text{m}$ ). – B1: TS – B2: TLS – B3: RLS. – Scale bars = 100  $\mu\text{m}$ .

sample resulting in several virtual thin sections. Finally, X-ray Computed Tomography at very high resolution (*i.e.* nanoCT) can be used to visualise charcoalified features that are obscured for example by mineral deposits that make visualising using SEM and HT- $\mu\text{CT}$  difficult. A directed search in nanoCT volumes allows localisation of ‘veiled’ features such as inter vessel pits under coated surfaces.

Identifying and evaluating such problems in combination with the implementation of complementary imaging techniques serve to strengthen interpretations pertaining to past ecosystems and cultures based on studies of charcoalified material.

## ACKNOWLEDGEMENTS

We are indebted to the Special Research Fund of Ghent University for financing the PhD project of Wannes Hubau. We thank the Commission for Scientific Research (Faculty of Bioscience Engineering, Ghent University) and the King Leopold III Fund for financially supporting the fieldwork. Furthermore, we thank the World Wide Fund for Nature (WWF), the École Régionale Post-universitaire d'Aménagement et de gestion Intégrés des Forêts et Territoires Tropicaux (ERAIFT, DR Congo) and the Institut National pour l'Étude et la Recherche Agronomique (INERA, DR Congo) for organisational and logistic support. Specifically, we thank Geert Lejeune and Bruno Pérodeau for their services and discussions in the field and all WWF-eco-guards who guided us through the Luki reserve. We thank the Royal Museum for Central Africa (Tervuren, Belgium) for financing radiocarbon dating and for organising the SEM sessions.

## REFERENCES

- African Plants Database. 2012. African Plants Database Version 3.3.3, Conservatoire et Jardin botaniques de la Ville de Genève and South African National Biodiversity Institute, Pretoria. Published on the internet [accessed 1st February 2011–10th August 2012], from <<http://www.ville-ge.ch/musinfo/bd/cjb/africa/>>.
- Angyalossy V, Angeles G, Pace MR, Lima AC, Dias Leme CL, Lohmann LG & Madero-Vega C. 2011. An overview on the anatomy, development and evolution of the vascular system of lianas. *Plant Ecol. & Divers.* 5: 1–16.
- Ascough PL, Bird MI, Francis SM, Thornton B, Midwood AJ, Scott AC & Apperley D. 2011. Variability in oxidative degradation of charcoal: Influence of production conditions and environmental exposure. *Geochim. et Cosmochim. acta* 75: 2361–2378.
- Bird MI, Ascough PL, Young IM, Wood CV & Scott AC. 2008. X-ray microtomographic imaging of charcoal. *J. Archaeolog. Sci.* 35: 2698–2706.
- Boutain JR, Brown AR, Webb DT & Toyofuku BH. 2010. Simplified procedure for hand fracturing, identifying, and curating small macrocharcoal remains. *IAWA J.* 31: 139–147.
- Braadbaart F & Poole I. 2008. Morphological, chemical and physical changes during charcoalification of wood and its relevance to archaeological contexts. *J. Archaeolog. Sci.* 35: 2434–2445.
- Brabant L, Vlassenbroeck J, De Witte Y, Cnudde V, Boone M, Dewanckele D & Van Hoorebeke L. 2011. Three-dimensional analysis of high-resolution X-ray computed tomography data with Morpho+. *Microscopy and Microanalysis* 17: 252–263.
- Burkill HM. 1985. The useful plants of West Tropical Africa. Ed. 1, 6 Vol. Royal Botanic Gardens, Kew, UK.
- Carcaillet C & Thion M. 1996. Pedaanthracological contribution to the study of the evolution of the upper treeline in the Maurienne Valley (North French Alps): methodology and preliminary data. *Rev. Palaeobot. Palynol.* 91: 399–416.
- Carlquist S. 1988. Comparative wood anatomy. Springer Verlag, Berlin, Heidelberg, Germany.
- Carlquist S. 1991. Anatomy of vine and liana stems: a review and synthesis. In: Putz RE & Mooney H (eds.), *The biology of vines*: 53–71. Cambridge University Press, Cambridge, UK.
- Chabal L, Fabre L, Terral J-F & Théry-Parisot I. 1999. L'anthracologie. In: Bourquin-Mignot C, Brochier J-E, Chabal L, *et al.* (eds.), *La botanique*: 43–104. Errance, Paris, France.
- Colombaroli D & Verschuren D. 2010. Tropical fire ecology across the African continent: A paleoecological perspective. *Pages News* 18: 65–67.
- Di Pasquale G, Marziano M, Impagliazzo S, Lubritto C, De Natale A & Bader MY. 2008. The Holocene tree line in the northern Andes (Ecuador): First evidence from soil charcoal. *Palaeogeog., Palaeoclimat., Palaeoecol.* 259: 17–34.

- Dias Leme CL, Cartwright C & Gasson P. 2010. Anatomical changes to the wood of *Mimosa ophthalmocentra* and *Mimosa tenuiflora* when charred at different temperatures. *IAWA J.* 31: 333–351.
- Dierick M, Van Loo D, Masschaele B, Boone MN & Van Hoorebeke L. 2010. A LabVIEW (R) based generic CT scanner control software platform. *J. X-ray Sci. & Technol.* 18: 451–461.
- Figueiral I & Mosbrugger V. 2000. A review of charcoal analysis as a tool for assessing Quaternary and Tertiary environments: achievements and limits. *Palaeogeog., Palaeoclimat., Palaeoecol.* 164: 397–407.
- Gale R & Cutler D. 2000. *Plants in archaeology*. Westbury Publishing, Otley, UK.
- Gasson P. 1987. Some implications of anatomical variations in the wood of pedunculate oak (*Quercus robur* L.) including comparison with common beech (*Fagus sylvatica* L.). *IAWA Bull. n.s.* 8: 149–166.
- Höhn A & Neumann K. 2012. Shifting cultivation and the development of a cultural landscape during the Iron Age (0–1500 AD) in the northern Sahel of Burkina Faso, West Africa: Insights from archaeological charcoal. *Quat. Internation.* 249: 72–83.
- Hubau W, Van den Bulcke J, Mees F, Van Acker J & Beeckman H. 2012. Charcoal identification in species-rich biomes: A protocol for Central Africa optimised for the Mayumbe forest. *Rev. Palaeobot. Palynol.* 171: 164–178.
- IAWA Committee. 1989. IAWA list of microscopic features for hardwood identification. *IAWA Bull. n.s.* 10: 219–332.
- InsideWood. 2012. The InsideWood Working Group (IWG), 2004-onwards. Published on the Internet [accessed 1st February 2012–10th August 2012], from <<http://insidewood.lib.ncsu.edu/search>>
- Lebrun J & Gilbert G. 1954. Une classification écologique des forêts du Congo. Publications de l'Institut National pour l'Étude Agronomique du Congo Belge (INEAC). Série scientifique 63. Bruxelles, Belgique.
- Mabberley DJ. 2008. *The plant-book*. Cambridge University Press, Cambridge, UK.
- Mannes D, Marone F, Lehmann E, Stambanoni M & Niemi P. 2010. Application areas of synchrotron radiation tomographic microscopy for wood research. *Wood Sci. & Technol.* 44: 67–84.
- Masschaele BC, Cnudde V, Dierick M, Jacobs P, Van Hoorebeke L & Vlassenbroeck J. 2007. UGCT: New X-ray radiography and tomography facility. *Nuclear Instruments and Methods in Physics Research Section A: Accelerators, Spectrometers, Detectors and Associated Equipment* 580: 266–269.
- Ngomanda A, Chepstow-Lusty A, Makaya M, Favier V, Schevin P, Maley J, Fontugne M, Oslisly R & Jolly D. 2009. Western equatorial African forest-savanna mosaics: a legacy of late Holocene climatic change? *Climate of the Past* 5: 647–659.
- Normand D & Paquis J. 1976. *Manuel d'identification des bois commerciaux*. Tome 2 Afrique guinéo-congolaise. Centre Technique Forestier Tropical, Nogent-sur-Marne, France.
- Picornell Gelabert L, Asouti E & Allué Martí E. 2011. The ethnoarchaeology of firewood management in the Fang villages of Equatorial Guinea, central Africa: Implications for the interpretation of wood fuel remains from archaeological sites. *J. Anthropolog. Archaeol.* 30: 375–384.
- Prior J & Gasson P. 1993. Anatomical changes on charring six African hardwoods. *IAWA J.* 14: 77–86.
- Scheel-Ybert R. 2000. Vegetation stability in the Southeastern Brazilian coastal area from 5500 to 1400 14C yr BP deduced from charcoal analysis. *Rev. Paleobot. Palynol.* 110: 111–138.
- Schweingruber FH. 1976. Veröffentlichungen über Untersuchungen prähistorischer Hölzer und Holzkohlen. *Cour. Forsch. Int. Senckenberg.* 17: 29–58.

- Schweingruber FH. 2007. Wood structure and environment. Springer Series in Wood Science. Springer-Verlag, Heidelberg, Germany.
- Schweingruber FH. 2012. Microtome sessions of charcoal. Technical note. IAWA J. 33: 327–328.
- Scott AC. 2000. The Pre-Quaternary history of fire. *Palaeogeog., Palaeoclimat., Palaeoecol.* 164: 281–329.
- Scott AC & Glasspool IJ. 2007. Observations and experiments on the origin and formation of inertinite group macerals. *Internat. J. Coal Geol.* 70: 53–66.
- Tervuren Xylarium Wood Database. 2012. Tervuren Wood Collection database of the Royal Museum for Central Africa. RMCA, Tervuren, Belgium. Published on the internet [accessed 1st February 2011–10th august 2012], from <http://www.africamuseum.be/collections/browsecollections/naturalsciences/earth/xylarium>
- Théry-Parisot I, Chabal L & Chravzez J. 2010. Anthracology and taphonomy, from wood gathering to charcoal analysis. A review of the taphonomic processes modifying charcoal assemblages, in archaeological contexts. *Palaeogeog., Palaeoclimat., Palaeoecol.* 291: 142–153.
- Van den Bulcke J, Boone M, Van Acker J, Stevens M & Van Hoorebeke L. 2009. X-ray tomography as a tool for detailed anatomical analysis. *Ann. Forest Sci.* 66: 508.
- Vlassenbroeck J, Dierick M, Masschaele B, Cnudde V, Van Hoorebeke L & Jacobs P. 2007. Software tools for quantification of X-ray microtomography at the UGCT. *Nuclear Instruments and Methods in Physics Research Section A: Accelerators, Spectrometers, Detectors and Associated Equipment* 580: 442–445.
- Wheeler EA. 2011. InsideWood - a web resource for hardwood anatomy. *IAWA J.* 32: 199–211.
- Wheeler EA, Baas P & Rodgers S. 2007. Variations in dicot wood anatomy. A global analysis based on the InsideWood database. *IAWA J.* 28: 229–258.

*Accepted: 10 January 2013*

*Associate Editor: Imogen Poole*